J Mater Sci (2007) 42:7794–7800
DOI 10.1007/s10853-007-1632-8

Welding of Al-359/20%SiC_p metal matrix composites by the novel MIG process with indirect electric arc (IEA)

Rafael García · Victor H. López · Andrew R. Kennedy · Gabriel Arias

Received: 10 October 2006 / Accepted: 20 February 2007 / Published online: 3 June 2007

Abstract An Al-based composite reinforced with 20%SiC_p was welded using the MIG welding process with direct and indirect application of the electric arc (DEA and IEA respectively). The welds were made on 12.5 mm thick plates in three welding passes for the DEA joint whereas only one pass was required for the IEA joint. Microstructural examination of the joints revealed DEA welds with light signs of matrix/reinforcement reaction whilst in the IEA welds the SiC particles remained with their initial angular morphology. Mechanical failure occurred consistently and independently of the type of joint in the weld zone and the measured strengths were 209 and 234 MPa for DEA and IEA welds respectively. The greater strength measured for the IEA weld was due to reduced porosity and good incorporation and dispersion of the SiC particles into the weld pool.

Introduction

Significant improvements in the properties of monolithic materials, such as Al and Al alloys, can be obtained by incorporating a hard and stiff ceramic phase as a reinforcement giving rise to a metal matrix composite (MMC). Vigorous research has led to developing suitable, scaleable and affordable processing methods to incorporate ceramics into metallic matrices, most of which involve a molten metal. Nowadays the MMCs technology is mature and a well established industry so that MMCs are found in a wide range of commercial applications [1]. Further spreading in exploiting the benefits of mixing metals and ceramics has been, however, slowed down by problems encountered in the secondary processing of this class of materials. The presence of a second phase brings added complications in these processes. For instance, conventional fusion welding produces a weld pool that has poor fluidity and solidifies with large volumes of porosity in the weld and heat affected zone (HAZ) depending on the processing method for the composite. The thermal stability of the reinforcing phase may be another concern [2].

Owing to its properties, availability and cost, SiC has been preferred to reinforce Al and its alloys. It has been found, however, to be thermally unstable in liquid Al at the processing temperatures, forming undesirable Al_4C_3 plus free Si. To overcome this problem significant quantities of Si are added [3–6]. Fusion welding of Al–Si/SiC composites has been found very problematic in terms of reactivity owing to the severe thermal cycle developed during arc welding. In the open literature, the formation of Al_4C_3 has repeatedly been reported in the weld metal in Al-based composites reinforced with SiC independently of the fusion welding process employed (laser and electron beam, TIG or MIG) [2, 7–9]. Only partial success has been observed in precluding the formation of Al_4C_3 by using low heat input levels and a fast thermal cycle with a laser even when the matrix is a Si-containing alloy [7, 8]. Previous studies [10, 11] demonstrated that the use of the MIG process with indirect electric arc is a suitable technique to weld both

R. García (✉) · V. H. López · G. Arias
Instituto de Investigaciones Metalúrgicas, Universidad Michoacana de San Nicolás de Hidalgo, A.P. 888, Morelia, C.P. 58 000, Michoacan, Mexico
e-mail: rgarcia@jupiter.umich.mx

A. R. Kennedy
Advanced Materials Research Group, School of Mechanical, Materials and Manufacturing Engineering, University of Nottingham, Nottingham NG7 2RD, UK

Al-alloys and Al-based composites with low and high contents of reinforcement. The present study aims to assess the possibility to produce sound welds of Al-359/20%SiCp composites through this novel method.

Experimental procedure

The parent material used in this study was an Al-359/20%SiC_P MMC (commercially known as F3S.20S) with an average particle size of 15 μm. Slices of the composite were cut from an ingot and machined to obtain plates of 12.5 × 40 × 130 mm. The design of the joints and their dimensions are shown in Fig. 1. For welding, an ER4043 electrode, 1.2 mm in diameter, was employed. Plates (10 × 5 × 140 mm) of Al-7 wt.% Si were used as feeding metal for MIG welding with IEA, as illustrated in the schematic drawing in Fig. 2. The chemical composition of the metallic materials employed and the welding parameters are listed in Tables 1 and 2 respectively. Welding current and voltage were adjusted to have a droplet spray transfer mode. Previous work revealed that to accomplish joining of either metal matrix composites or monolithic materials by the IEA technique, preheating of the base materials is a requisite [10–13]. The IEA joint was, therefore, preheated to 100°C in this study whilst the DEA joint was welded at ambient temperature. A travel speed of

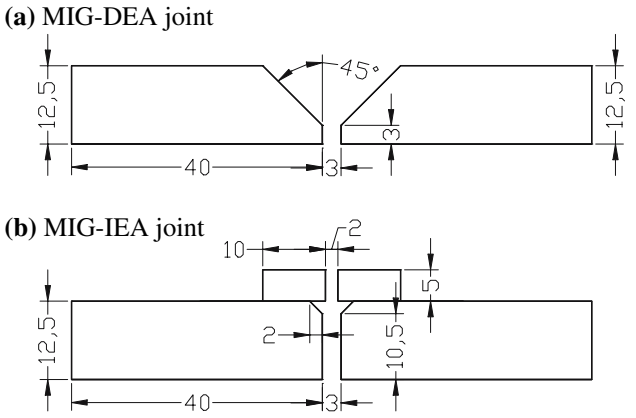

Fig. 1 Joint design and dimensions (mm) when the electric arc is applied (**a**) directly and (**b**) indirectly

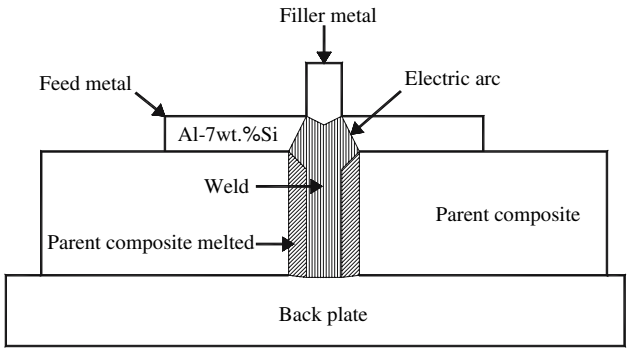

Fig. 2 Schematic of the MIG-IEA welding process with indirect electric arc

3.6 mm s^{-1} was found to be suitable for filling the joint gap of the IEA joint and succeed lateral fusion with a sole welding pass. The same travel speed produced a DEA welded joint with a reasonable reinforcement. On this basis, the same welding speed was used for both joints so as to have comparable heat inputs per welding pass. It is worth noting that joint preparation in single V-groove and three welding passes were required for the DEA weld whilst for the IEA weld only one pass was needed. Thus the heat input to the IEA joint is approximately 1/3 of the total heat input to the DEA joint.

In order to reveal and examine the microstructure in the welded joints, standard metallographic techniques were used to prepare the samples but the use of the water was omitted in order to avoid the removal of any Al_4C_3 that might have been present. Microstructural characterisation was performed by means of an optical microscope (OM) and a scanning electron microscope (SEM) attached to an energy dispersive X-ray spectroscopy (EDX) system. X-ray diffraction (XRD) was used to identify the phases present in the welds by using CuK_α radiation for 2θ values between 20 and 70° with a scanning step of 0.02°. Transversal hardness weld profiles were generated by applying a 500 grams load with a Vickers indent for 10 s. Indentation lines were carried out at approximately half of the weld height on mirror-like polished samples. Tensile tests were carried out, at room temperature, on a universal testing machine at a cross head speed of 0.083 mm s^{-1}.

Table 1 Chemical composition of the metallic materials employed (%wt.)

Material	% Al	% Si	% Fe	% Cu	% Mn	% Mg	% Cr	% Ni	% Zn	% Ti
ER4043	Bal.	5.25	0.8	0.3	0.05	0.05	–	–	0.10	0.02
A-359	Bal.	9.3	0.11	0.01	<0.01	0.55	–	–	<0.01	<0.02
Al–Si*	Bal.	7.12	0.02	0.001	0.01	0.001	0.01	0.001	0.001	<.01

* Feeding strips

Table 2 MIG welding parameters using DEA and IEA

Parameter	Value
Current (A)	230 (IEA)/220 (DEA)
Voltage (V)	21
Travel speed (mm s^{-1})	3.6
Argon flow rate (l min^{-1})	22
Pre-heating temperature (°C)	100 (IEA)/25 (DEA)
Heat input (kJ s^{-1})	1.34 (IEA)/1.28 (DEA)*
Stick out	12 mm

*Per welding pass

Results and discussion

Geometry of the welds

Typical cross section profiles of the welds obtained by means of DEA and IEA are compared in Fig. 3. These macrographs were used to calculate the dilution of base composite as indicated in [12] and the values were found to be 32% and 48.9% for DEA and IEA respectively. Besides, the area fraction measurements from Fig. 3 were used to estimate that the true heat input to the base composite for the IEA joint was approximately 1.14 kJ s^{-1} (considering a thermal efficiency of 94.8% [12] and a fraction of 9.84% of heat absorbed by the feeding strips) whereas the true heat input to the base composite for the DEA joint was approximately between 2.88 and 3.07 kJ s^{-1} (considering the thermal efficiency between 75 and 80%). Thus it is clear that the actual thermal affection suffered by the base composites is approximately a factor of three larger for the DEA joint than for the novel IEA joint.

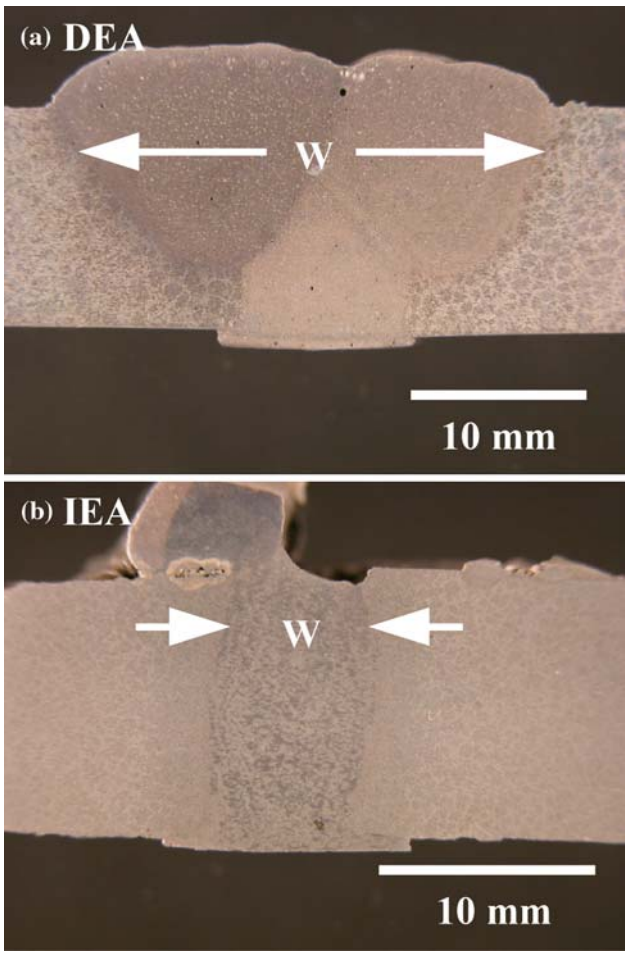

Fig. 3 Profiles of the welds deposited by (**a**) DEA at room temperature and (**b**) IEA at 100 °C

The arrows in Fig. 3 indicate the widths of the welds in the top of the welded joint. The width of the IEA weld varied between 5 and 7 mm whereas the DEA weld had approximately 10 mm and 28 mm in the bottom and top respectively. The three welding passes required for the DEA joint are clearly delineated in Fig. 3a) and the presence of macroporosity mainly in the upper part of the weld bead is also observed. The use of the IEA technique resulted in an uniform weld profile, as shown in Fig. 3b), in which full penetration without lack of lateral fusion was achieved with only one welding pass by pre-heating the joint to 100 °C. Very little macroporosity was observed. It was demonstrated in a previous work [12], that the used of IEA improves the thermal efficiency of the MIG process, due to the hidden establishment of the electric arc (Fig. 2.) which minimises heat losses and reduces the lateral extent of fusion in the based material and therefore the HAZ, enabling thus welding of thick plates in one welding pass. It is worthy bearing in mind that most of the attempts to weld MMCs have been performed rather in thin sections or making bead on plate welds [2, 7–9] and a number of welding passes have been typically applied to succeed welding of sections thicker than 6 mm [14], as required in this study for the MIG-DEA process. A possible disadvantage of the MIG-IEA welded joints could be envisaged, that is the presence of the feeding strips after welding. This feature should not be considered as a big handicap for using the IEA joint since the residual feeding strips can be easily removed and in some cases they detach themselves during welding. That was the case for the right side of the weld shown in Fig. 3b).

Microstructure

Figure 4 shows the characteristic microstructure of the as received Al-359/20%SiC_P MMC. It can be observed that the SiC particles are reasonably well distributed although they are allocated at the converging dendrite arms in the intercellular regions along with eutectic silicon, Al–Si–Fe and Al–Si–Fe–Mg precipitates clearly delineating the cell boundaries. Also some levels of porosity are appreciated

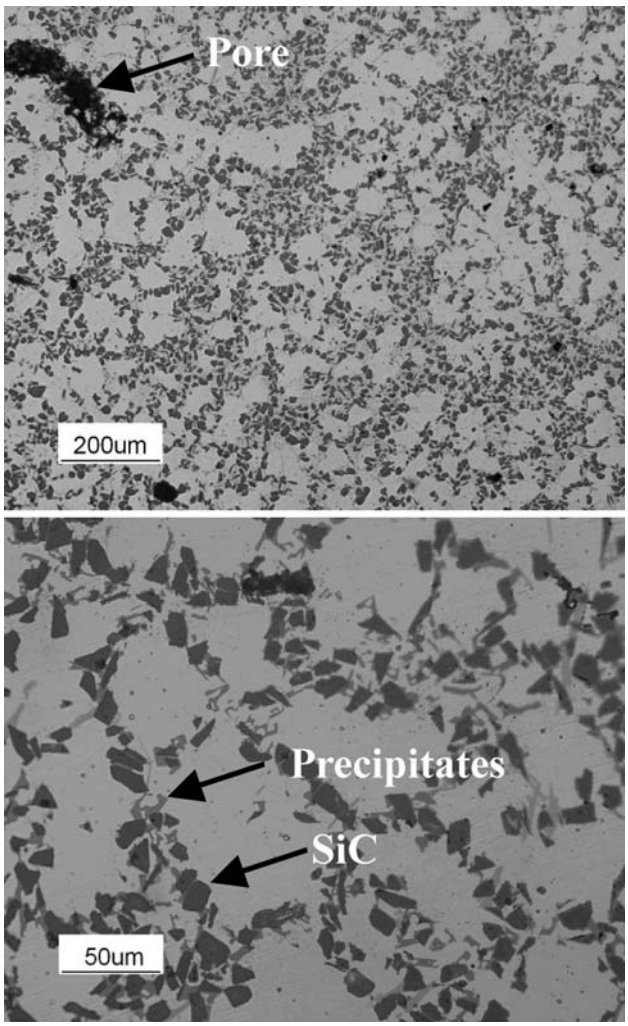

Fig. 4 Typical microstructure of the as-received MMC

ranging from macro to micropores. A detailed examination did not reveal signs of reaction between the matrix and the reinforcement, i.e. the outlines of the SiC particles are sharp and angular.

Figure 5 shows the microstructure obtained by IEA at the bottom of the weld. It is clear that a significant amount of SiC particles were incorporated and dispersed into the weld pool as a result of an even fusion along the height of the sidewalls of the working pieces. An estimation through image analysis roughly indicated levels of reinforcement in the weld metal of 12 vol.%. This level of reinforcement in the weld metal is quite consistent with the dilution of base composite estimated for this joint. The presence of porosity in the weld is also visible. As the pores are similar to those observed in the base metal and since they are allocated mainly in the neighbourhood of the fusion line, it is believed that a significant fraction of this porosity was dragged from the sidewalls of the base composite. Along the height of the weld there were no signs of lack of fusion in the base composite and there was, therefore, continuity between the weld metal and the matrix of the composite as can be seen in Fig. 6 at larger magnifications. Three zones can be distinguished in this image; the base composite (BC), a partially melted zone (PMZ, which is approximately 420 μm wide) and the weld metal. Whilst the fusion line and PMZ are characterised by the agglomeration of very fine precipitates in the grain boundaries (Fig. 7a), which give the appearance of coarsening in Fig. 6, the weld metal exhibits a refined cellular dendritic structure (Fig. 7b). Such a refinement is caused by the high cooling rates [3, 15] experienced in the weld pool and the size of the cells is approximately the size of the SiC particles. It has been, however, observed that the cell size is not determined by the presence and size of the SiC particles [3, 15]. In this case (Fig. 7), the SiC particles are also trapped between converging dendrites during solidification.

Dissolution of the SiC particles, is typically characterised by the presence of elongated Al_4C_3 or Al_4SiC_4 needles when the reaction is severe or by the nucleation and growth of Al_4C_3 blocks on the surface of the SiC particles when the reaction is moderate. Microstructural observations in the OM and SEM did not reveal any of these signs of reaction in the weld metal and neither in the HAZ. In Fig. 7, it can be observed that the SiC particles retained,

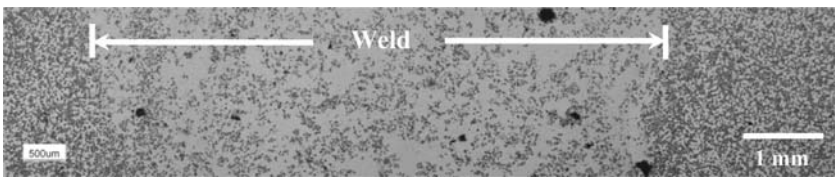

Fig. 5 Microstructure at the bottom of the MIG-IEA weld

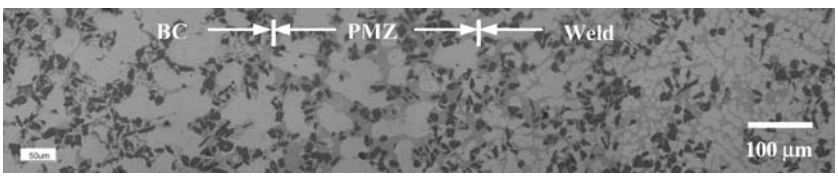

Fig. 6 Typical microstructure at the base metal/weld interface in a MIG-IEA weld

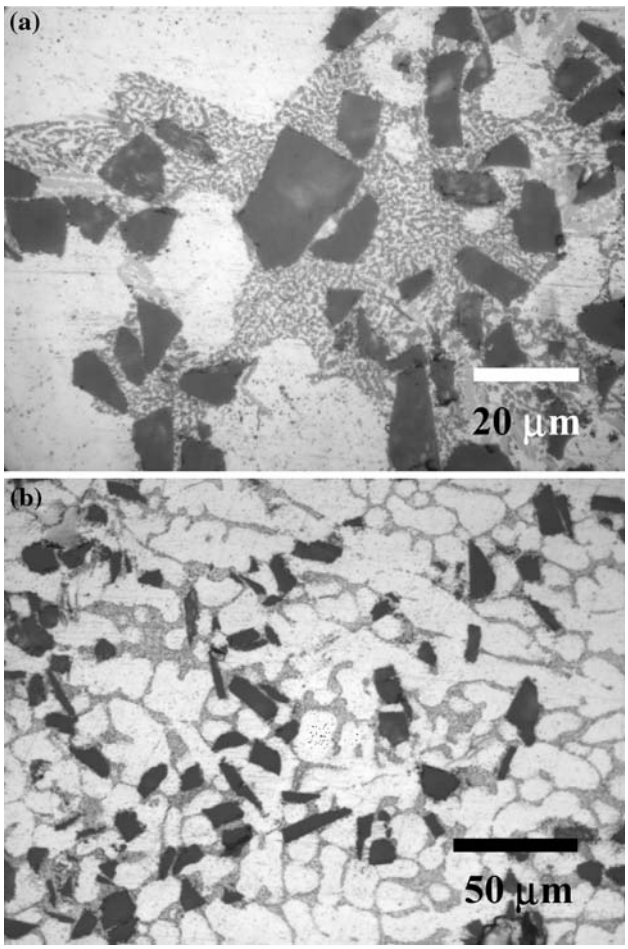

Fig. 7 Microstructural characteristics of a MIG-IEA weld at: (**a**) the interface and (**b**) weld centre

after the severe but rapid welding thermal cycle, their initial sharp and angular morphology.

Further analysis by XRD confirmed this fact as shown in Fig. 8 in which the corresponding reflections for SiC, Si and Al are only present along with reflections of low intensity of intermetallics. The plot in Fig. 8 also shows the XRD pattern of the MIG-DEA weld. Generally speaking, no appreciable difference between them can be pointed out, except the larger intensity of the main reflection peaks for Si and SiC in the IEA weld due to the use of the Al-7 wt.%Si feeding strips and the significant incorporation of SiC particles into the weld pool for the IEA weld. The microstructural differences can be, however, revealed by looking at the optical micrographs shown in Figs. 9 and 10. First of all, a large fraction of the MIG-DEA weld was denuded of SiC particles, mainly the second and third welding passes, and where there was the presence of SiC particles, they were clustered. A larger volume of macro and microporosity was also observed and the width of the PMZ was approximately 4500 μm in the mid height of the weld.

Whilst no reactivity signs were observed at the weld/base metal interface (Fig. 9a), the particles quite evenly distributed in the root pass and clustered in the top of the weld,

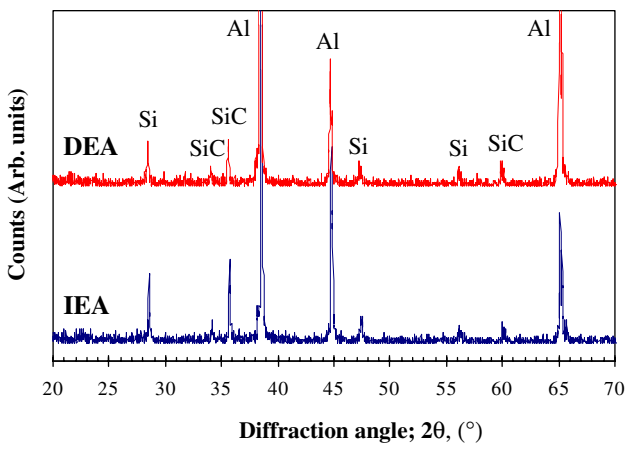

Fig. 8 XRD patterns of the welds obtained by IEA and DEA

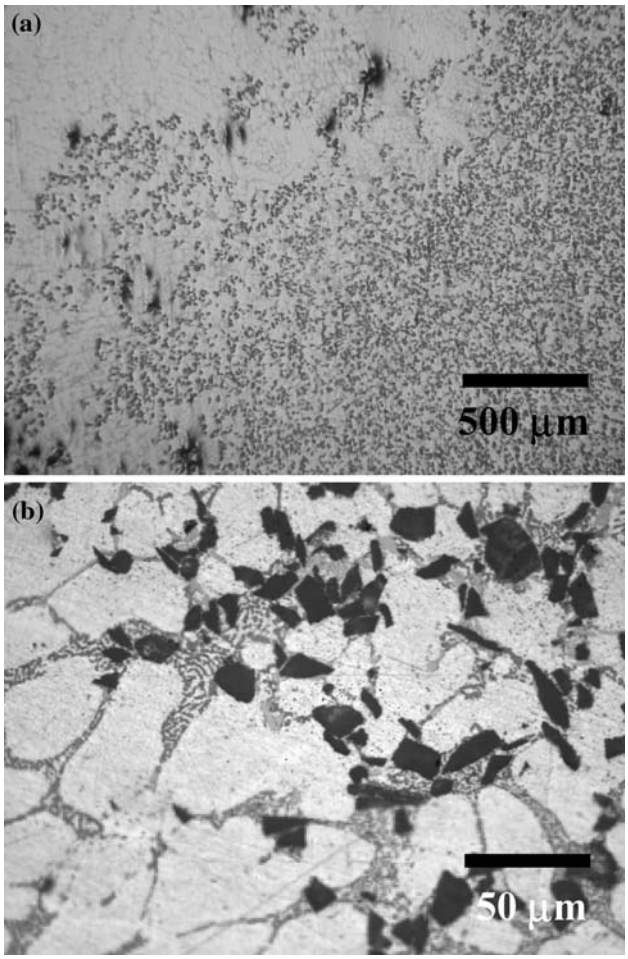

Fig. 9 Microstructure of a MIG-DEA weld at the base metal/weld interface. (**a**) low and (**b**) high magnifications

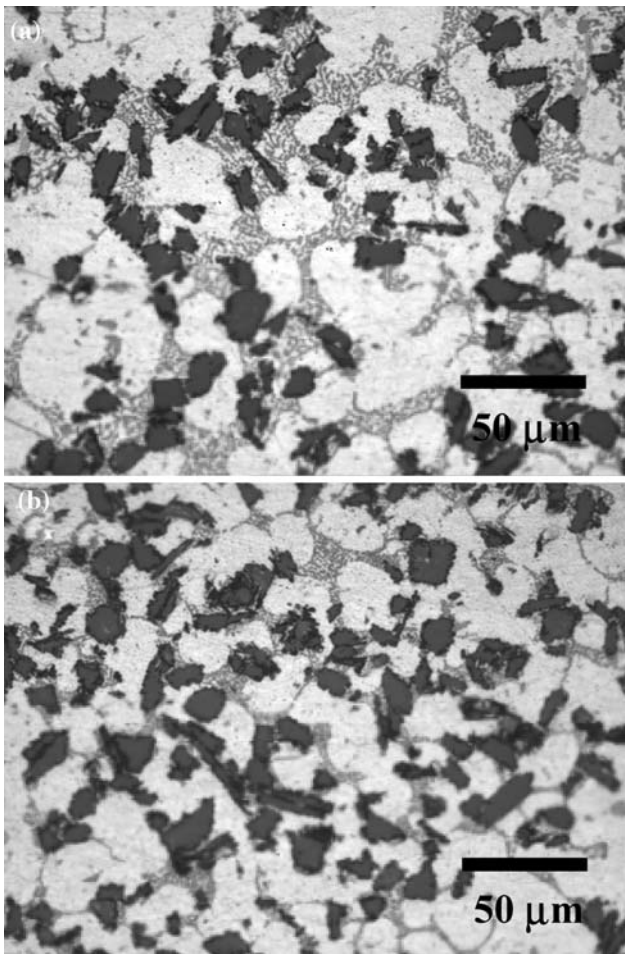

Fig. 10 Microstructure of a MIG-DEA weld at: (**a**) the root pass and (**b**) the top of the weld

exhibited jagged contours. This morphological alteration clearly indicates that moderate reaction took place during welding and the levels of the SiC dissolution to form Al_4C_3 are very low to be detected by XRD.

The Al–SiC system has been thoroughly studied and its thermodynamics is well established [3–6]. Between 650 and 1323 °C, SiC reacts with Al according to the reaction

$$4Al + 3SiC \rightarrow Al_4C_3 + 3Si$$

and the kinetics of the reaction increases with temperature. Above 1323 °C and up to 1627, another reaction takes place leading to the formation of Al_4SiC_4. If the temperature increases further the ternary carbide Al_8SiC_7 precipitates [3–6]. To preclude the decomposition of SiC with Al, increasing contents of Si are required as a function of temperature. For the welds of this study, the content of Si is between 9.5 and 5.5 wt.% with the value for the IEA welded joint being slightly higher than for the DEA weld. Considering the upper limit, for a Si content of 9.5 wt.% thermodynamics predicts that SiC is unstable approximately above 890 °C [4, 6]. That temperature was far exceeded in the weld pool during welding. However, in none of the welds bulk dissolution of the SiC particles was seen. The rapid thermal cycle of welding and the relatively high content of Si in the weld pool, which slows down the kinetics of the dissolution reaction [6], account for this fact. The light reaction observed in the DEA joint occurred due to the direct exposition of the base composite to the high temperatures of the electric arc and the high heat input in a small volume of material as highlighted in section ''Geometry of the welds''. On the counter side, in the IEA joint the electric arc is indirectly established, in a hidden manner, on the Al-7 wt.%Si feeding strips forming a weld pool which feeds the gap joint with liquid at high temperature and the heat input is dissipated or absorbed by a larger volume of material. This fusion joining mechanism reduces the thermal affection of the joint and prevents, at least to the resolution of the SEM, chemical interactions between the Al–Si liquid and the SiC particles, facilitating fusion welding of thick sections.

Mechanical properties and fracture

Figure 11 shows transverse microhardness profiles carried out on welds deposited by both methods, DEA and IEA. Accordingly to the macrographs shown in Fig. 3, a comparison between DEA and IEA hardness profiles shows that the DEA weld is wider than the IEA. It is also noticeable that average hardness values, within the welds, are similar for both joints. The dramatic increase in hardness observed by others [2, 7] as a result of severe dissolution of SiC was not observed in this study.

Regarding tensile testing, mechanical failure occurred consistently in the weld zone for both methods and the measured ultimate tensile strengths (UTS) were 209 and

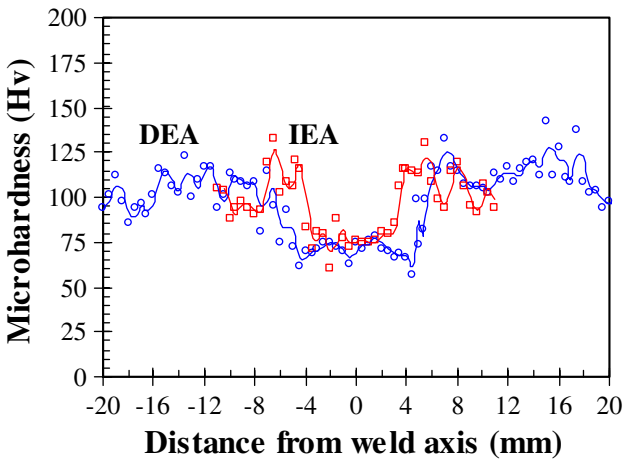

Fig. 11 Transverse microhardness profiles for DEA (circles) and IEA (squares) welds

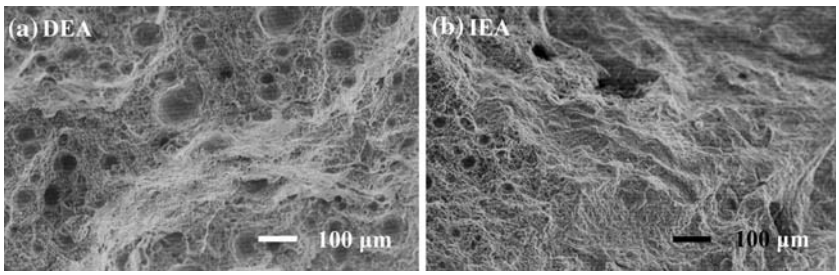

Fig. 12 Fracture surfaces of tensile specimens

234 MPa for welds with the direct and indirect application of the electric arc respectively. Considering that the UTS for the filler wire and parent composite are 190 and 262 MPa respectively, it seems that the strength of the DEA and IEA weldments is related to the strength of filler wire and parent composite respectively. Figure 12 shows the fracture characteristics exhibited by the welds after mechanical failure under tension. These fractographies evidence the larger levels of porosity for the DEA weld in which it is clear that the fracture path was dictated by these defects. For the MIG-IEA weld, the features observed at higher magnifications revealed particle-matrix debonding and voiding as well as cracking of intermetallics associated to the SiC particles. These are the typical failure mechanisms found by others in Al–Si/SiC MMCs [3, 9]. The fact that the failure occurred in the weld, is an indication of the good bonding achieved at the weld/composite interface, irrespective of the method of welding employed. Thus the relatively high content of ceramic is not an obstacle for welding this type of composite and the highest strength obtained for the MIG-IEA weld was due to the reduced levels of porosity and larger incorporation of SiC particles into the weld metal. The light reaction of the SiC particles in the DEA joint probably played a minor role in the mechanical behaviour of this weld. In the long term, the MIG-IEA weld guaranties a better performance as reaction was not observed contrary to the MIG-DEA weld in which the moderate presence of Al_4C_3 will make it prone to corrosion in moist environments.

Conclusions

Thick plates of Al-359/20%SiC_p metal matrix composites were successfully welded using the MIG welding process with the direct and indirect application of the electric arc. For the DEA joints it was necessary to deposit three weld beads whilst for the IEA joint one deposit was sufficient to join the plates. The IEA led to welds with reduced porosity, nonvisible signs of reaction and a larger incorporation and fairly good dispersion of SiC particles into the weld pool. These characteristics were reflected in a greater tensile strength of 234 MPa as compared to 209 MPa for the DEA welds in which little incorporation of the SiC particles into the weld occurred with moderate dissolution of the clustered SiC particles to form Al_4C_3. The larger porosity of the DEA welds was determinant in its failure during tensile testing. Thus the MIG-IEA technique appears as a good alternative for fusion welding of Al–Si/SiC composites with a minimal thermal affection.

Acknowledgements The authors would like to thank Coordinación de la Investigación Científica of the UMSNH for funding this study and to Juan Jose Uribe Galan from Instituto Tecnologico de Morelia for the facilities consented in the use of the Mitutoyo video line indenter.

References

1. Miracle DB (2005) Compos Sci Technol 65:2526
2. Ahearn JS, Cooke C, Fishman SG (1982) Met Constr 14:192
3. Lloyd DJ (1989) Compos Sci Technol 35:159
4. Viala JC, Fortier P, Bouix J (1990) J Mater Sci 25:1842
5. Viala JC, Bosselet F, Laurent V, Lepetitcorps Y (1993) J Mater Sci 28:5301
6. Aksenov AA, Belov NA, Medvedeva SV (2001) Z Metallkd 92:1103
7. Lienert JT, Brandon ED, Lippold JC (1993) Scripta Metall Mater 28:1341
8. Bonollo F, Tiziani A, Penasa M (2002) Int J Mater Product Technol 17:291
9. Ureña A, Escalera MD, Gil L (2000) Compos Sci Technol 60:613
10. Garcia R, Lopez VH, Bedolla E, Manzano A (2002) J Mater Sci Let 21:1965
11. Garcia R, Lopez VH, Bedolla E, Manzano A (2003) J Mater Sci 38:2771
12. Garcia R, Lopez VH (2006) J Mater Sci, doi:10.1007/s10853-006-1287-x
13. Natividad C, Salazar M, Garcia R, Gonzalez-Rodriguez JG, Perez R (2006) Corrosion Eng Sci Technol 41:91
14. Altshuller B, Christy W, Wiskel B (1990) In: Patterson RA, Mahin KW (eds) Weldability of materials. ASM International, Detroit, Michigan, USA, 305 pp
15. Gowri S, Samuel FH (1992) Metall Trans A 23A:3369